Published in final edited form as:
*Free Radic Biol Med*. 2011 September 15; 51(6): 1146–1154. doi:10.1016/j.freeradbiomed.2011.05.041.

# 2′,5′-Dihydroxychalcone-induced glutathione is mediated by oxidative stress and kinase signaling pathways

**Remy Kachadourian**[a,c], **Subbiah Pugazhenthi**[b,c], **Kalpana Velmurugan**[b], **Donald S. Backos**[d], **Christopher C. Franklin**[d], **Joe M. McCord**[c], and **Brian J. Day**[a,c,d,*]

[a]Department of Medicine, National Jewish Health, Denver, CO 80206

[b]Denver VA Medical Center, Denver, CO 80220

[c]Department of Medicine, University of Colorado Denver, Aurora CO 80045

[d]Department of Pharmaceutical Sciences, University of Colorado Denver, Aurora CO 80045

## Abstract

Hydroxychalcones are naturally occurring compounds that continue to attract considerable interest due to their anti-inflammatory and anti-angiogenic properties. They have been reported to inhibit the synthesis of the inducible nitric oxide (NO) synthase and to induce the expression of heme oxygenase-1 (HO-1). This study examines the mechanisms by which 2′,5′-dihydroxychalcone (2′,5′-DHC) induces an increase in cellular glutathione (GSH) levels using a cell line stably expressing a luciferase reporter gene driven by antioxidant response elements (MCF-7/AREc32). 2′,5′-DHC-induced increase in cellular GSH levels was partially inhibited by the catalytic antioxidant MnTDE-1,3-IP$^{5+}$, suggesting that reactive oxygen species (ROS) mediate the antioxidant adaptive response. 2′,5′-DHC treatment induced the phosphorylation of c-Jun N-terminal kinase (JNK) pathway that was also inhibited by MnTDE-1,3-IP$^{5+}$. These findings suggest a ROS-dependent activation of the AP-1 transcriptional response. However, while 2′,5′-DHC triggered the NF-E2-related factor 2 (Nrf2) transcriptional response, co-treatment with MnTDE-1,3-IP$^{5+}$ did not decrease 2′,5′-DHC-induced Nrf2/ARE activity, showing that this pathway is not dependent on ROS. Moreover, pharmacological inhibitors of mitogen-activated protein (MAP) kinase pathways showed a role for JNK and p38MAPK in mediating the 2′,5′-DHC-induced Nrf2 response. These findings suggest that the 2′,5′-DHC-induced increase in GSH levels results from a combination of ROS-dependent and ROS-independent pathways.

### Keywords

ROS; Nrf2; AP-1; MCF-7/AREc32; metalloporphyrin

## Introduction

Hydroxychalcones (HCs) are both the biosynthetic precursors of flavonoids and end-products associated with a variety of biological activities [1–3]. Their anti-inflammatory and



*Corresponding author at: Department of Medicine, National Jewish Health, 1400 Jackson St. A439, Denver, CO 80206. Phone (303) 398-1121, Fax (303) 270-2168. dayb@njhealth.org.

anti-angiogenic properties continue to attract considerable interest [4,5]. Along with flavonoids, HCs can generate oxidative stress by interfering with the mitochondrial respiratory chain and by inducing glutathione (GSH) efflux through multi-drug resistance-associated proteins (MRPs) [6–8]. While flavonoids such as chrysin and apigenin induce GSH efflux through MRP1, HCs-induced GSH efflux is mediated by the breast cancer resistance protein (BCRP/ABCG2) [9–12]. Another relevant difference between HCs and chrysin is that HCs also appear to induce a rebound in intracellular GSH (iGSH) levels [13].

Cells adapt to increased levels of reactive oxygen species (ROS) by inducing the expression of a series of phase II antioxidant enzymes, including heme oxygenase-1 (HO-1) and the enzymes involved in the synthesis of GSH [14–16]. This antioxidant adaptive response is mediated by several transcriptional pathways, including NF-E2-related factor-2 (Nrf2) and activator protein-1 (AP-1) [17–19]. However, a number of protein kinase signaling pathways have been shown to trigger both the Nrf2 and AP-1 pathways independently from ROS overproduction [20,21]. Several studies have examined the mechanism of HCs-induced HO-1 expression, but not of HCs-induced GSH synthesis [22–25]. The non-hydroxylated chalcone (Fig. 1) has been shown to trigger the Nrf2-mediated response [22], and studies with 2′-hydroxychalcone (2′-HC, Fig. 1) have associated HO-1 expression with the phosphatidylinositol 3-kinase (PI3K) pathway and AP-1 activation [23–25]. The involvement of ROS in these pathways remains unclear.

The aim of this study was to examine the mechanisms by which 2′,5′-dihydroxychalcone (2′,5′-DHC, Fig. 1) induces elevated cellular levels of GSH using a transformed breast cancer cell line stably expressing a luciferase reporter gene driven by antioxidant response elements (MCF-7/AREc32). A powerful tool to study the involvement of oxidative stress in cellular processes is the catalytic antioxidant MnTDE-1,3-IP$^{5+}$, a member of a series of cationic manganese porphyrins that dismute superoxide and hydrogen peroxide, scavenge peroxynitrite and inhibit lipid peroxidation [26–28]. As shown using MnTDE-1,3-IP$^{5+}$, 2′,5′-DHC triggered a ROS-dependent activation of the JNK pathway, which was associated with both the AP-1- and Nrf2-mediated antioxidant transcriptional responses. However, the activation of the Nrf2/ARE pathway appeared to be independent from ROS and involved both JNK and p38MAPK pathways.

## Materials and methods

### Chemicals and reagents

Chalcone, 2′-hydroxychalcone (2′-HC), 2′,5′-dihydroxychalcone (2′,5′-DHC) were purchased from Indofine Chemicals Company, Inc (Hillsborough, NJ). Chrysin, L-buthionine sulfoximine (BSO), L-glutathione, pyruvate (sodium salt), ATP, acivicin, *N*-ethylmorpholine, phenylmethanesulfonyl fluoride (PMSF), sulfosalicylic acid, phosphoric acid, meta-phosphoric acid, sodium phosphate (monobasic), Triton X-100, EDTA, NADH, NADPH, $K_2HPO_4$, $KH_2PO_4$, HEPES, KCl, $MgCl_2$, sucrose, D-mannitol, DMSO and DMF were purchased from Sigma-Aldrich (St. Louis, MO). Tris-HCl, NaCl, 2-mercaptoethanol and methanol were purchased from Fisher (Pittsburgh, PA). SDS was purchased from Bio-Rad Laboratories (Hercules, CA). MitoSOX was obtained from Molecular Probes (Eugene, OR). Phosphate-Buffered Saline (PBS) was obtained from Cellgro (Herndon, VA). Protease inhibitor cocktail tablets supplemented with EDTA were obtained from Roche Diagnostics (Indianapolis, IN). SB203580, wortmannin and U0126 were purchased from Biomol (Plymouth Meeting, PA). SP600125 was purchased from Calbiochem (San Diego, CA). Manganese(III) *meso*-tetrakis(*N,N′*-diethylimidazolium-2-yl)porphyrin (MnTDE-1,3-IP$^{5+}$) was prepared as previously described in US patent #6,544,975B1 and was a kind gift from Aeolus Pharmaceuticals (Mission Viejo, CA).

### Cell lines and culture conditions

Transformed breast cancer cells stably expressing a luciferase reporter gene driven by antioxidant response elements (MCF-7/AREc32), referred to as AREc32 cells in this study, were obtained from Dr. C. Roland Wolf (University of Dundee, UK) and were grown in DMEM (low glucose) supplemented with 10% fetal bovine serum (FBS), 1% pen/strep (10,000 unit, Cellgro) and geneticin (400 mg/500 ml) at 37°C and 5% $CO_2$ supplemented air atmosphere [29]. 16HBE cells, a transformed human bronchial epithelial cell line, were grown in minimal essential medium α + Glutamax (Invitrogen, Carlsbad, CA) supplemented with 10% with FBS and 1% pen/strep. A Gal4 reporter system (Strategene, Lajolla, CA) was used to measure the transactivational activity of c-Jun as described previously [30]. This reporter assay uses a luciferase reporter gene driven by four copies of the Gal4 regulatory sequence (pGal4-TK-Luc) and an expression vector for the chimeric protein, Gal4-c-Jun which consists of the DNA-binding domain of Gal4 and the transactivation domain of c-Jun. Transient transfection of these plasmids in cultured 16HBE cells was carried out using LipofectAMINE 2000 reagent (Invitrogen-Life Technologies, Carlsbad, CA). A constitutively active renilla luciferase (pRL-TK-luc) was included to correct for transfection efficiency and to account for nonspecific effects of treatments on luciferase activity.

### Assessment of cytotoxicity

The 3-[4,5-dimethylthiazol-2-yl]-2,5-diphenyltetrazolium bromide (MTT) assay is commonly used to measure cancer cell survival, yet it has revealed artifacts when measuring the cytotoxicity of pro-oxidant agents [31]. Another simple method to evaluate drug-induced cytotoxicity is using membrane integrity as an index, which can be assessed by monitoring the release of cytosolic lactate dehydrogenase (LDH). AREc32 cells were grown in 24-well plates and LDH activity was measured after 48 h treatment in the culture medium and cell lysates (50 mM HEPES, 0.5% Triton X-100, pH 7) using a plate reader format as previously described [32]. Briefly, 5 μl of cell culture supernatant or lysates were incubated with 0.24 mM NADH in a Tris/NaCl pH 7.2 buffer in 96-well plates for 5 min at 25°C. The reaction was started by the addition of 9.8 mM pyruvate and the consumption of NADH was followed at 340 nm for 5 min at 30°C. Percent LDH release was calculated by the following equation: supernatant LDH/(supernatant LDH + lysate LDH) × 100.

### Flow cytometry and microscopy

MitoSOX is an analog of hydroethidine and is routinely used to detect mitochondrial ROS by flow cytometry [33]. The results obtained with this method remain qualitative rather than quantitative [34]. The oxidation products of MitoSOX were detected using the FL2 channel. Briefly, AREc32 cells were grown in 24-well plates and treated cells (approximately $5 \times 10^4$) were exposed to 5 μM MitoSOX for 20 min. The supernatant was removed and the cells scraped in 0.5 ml ice-cold PBS, centrifuged at 2,000 *g* for 15 min, and re-suspended in 0.5 ml ice-cold PBS. Cells were analyzed within 30 min using a FACS Calibur flow cytometer (Becton Dickinson Biosciences, San Jose, CA). The total number of gated cells counted was 10,000. Microscopy images were obtained directly from the culture plate following MitoSOX treatment and replacement of the culture media with PBS using an Evos-fl microscope (Advanced Microscopy Group, Bothell, WA).

### Intracellular levels of GSH

Intracellular GSH levels were determined by HPLC with electrochemical detection (HPLC-EC) [35]. Cultured AREc32 cells from 24-well plates were washed once with 1 ml of PBS, re-suspended in 0.5 ml of PBS and sonicated. 10% meta-phosphoric acid (25 μl) was then added to the samples (1% v/v final concentration), the samples centrifuged at 20,000 *g* for 10 min, and the supernatants used for HPLC analysis. The HPLC column used was a

Synergi 4u Hydro-RP 80A (150 × 4.6 mm) from Phenomenex (Torrance, CA) and the mobile phase was sodium phosphate buffer (125 mM sodium phosphate monobasic, pH adjusted to 3 with phosphoric acid) and 0.9% methanol. The flow rate was 0.5 ml/min. The retention time for GSH under these conditions was 7.0 min. The HPLC instrument was from ESA, Inc. (Chelmsford, MA), and was equipped with an autosampler (model 540) and a Coul array detector (model 5600A). The potential applied was + 0.75 V vs. H/Pd electrode, and the injection volume was 5 μl. The remaining 0.1 ml sample was used to measure protein content using Coomassie plus protein assay reagent (Thermoscientific, Rockford, IL).

### GCL activity from protein extracts

GCL activity was measured by analyzing γ-glutamylcysteine (γ-GC) production by HPLC as described previously [36]. AREc32 cells were grown in T-150 flasks and treated with 15 μM 2′,5′-DHC for 16 h. Cells were washed with cold PBS and scraped and sonicated in 0.25 M sucrose containing 1 mM EDTA, 20 mM Tris-HCl (pH 7.4), 50 μg/ml of PMSF and protease inhibitor cocktail, and sonicated. The samples were then centrifuged at 3000 × *g* for 10 min at 4°C and the supernatant was centrifuged at 10,000 *g* for 20 min and then, at 105,000 *g* for 30 min at 4°C. To remove endogenous inhibitors, acceptors and amino acids, the supernatant was centrifuged in microcon-10 (Amicon) tubes for 20–30 min at 4°C at 15,000 *g* and washed twice with 0.3 ml of the lysis solution (0.1 M Tris-HCl, pH 8.2, 150 mM KCl, 20 mM $MgCl_2$, and 2 mM EDTA). Final concentrates were tested for their protein content. The reaction was initiated by adding protein to the prewarmed (37°C) incubation mixture, which contained 20 mM glutamic acid, 5 mM cysteine, 10 mM ATP, 0.1 M Tris-HCl (pH 8.2), 150 mM KCl, 20 mM $MgCl_2$, 2 mM EDTA and 0.04 mg/ml of acivicin. Final protein concentration in the reaction mixture was between 0.1–1 mg/ml. After 30 min of incubation, 50 mM *N*-ethylmorpholine was added to bring pH of the reaction mixture to 8.5, then 5 mM monobromobimane was added. The derivatization was carried out in the dark for 30 min at room temperature. Sulfosalicylic acid (10%) was added after derivatization and the reaction mixture centrifuged at 10,000 *g* for 20 min. The supernatants (derivatized thiols) were analyzed by HPLC with fluorescence detection as described previously [36], using a Synergi 4-μM Hydro-RP 80A $C_{18}$ column (150 × 4.6 mm, Phenomenex, Torrance, CA), a mixture acetic acid/acetonitrile/water (1:8:91, pH 4.25) as mobile phase, a Hitachi HPLC instrument (model Elite LaChrom, Hitachi, San Jose, CA) coupled with a fluorometric detector (model L-2480) and a flow rate of 1 ml/min. Concentrations of γ-GC were measured using standard curves generated with known amounts of γ-GC. GCL activity was reported as nmol γ-GC/g protein/min.

### Immunoblotting of HO-1, GCLC, GCLM and GCL holoenzyme

AREc32 cells were grown in 24-well plates and, after treatment, washed with PBS. Cells were then sonicated in 200 μl of PBS. Cell debris was spun down and the supernatant volume reduced to approximately 30 μl by evaporation using a speed vacuum system. The resulting cytosolic proteins were resolved in a PAGEr® Gold Precast Polyacrylamide 4–20% Tris-Glycine gel (Cambrex Bio Science, Rockland, ME). Samples were run at 150 volts for 60 min and transferred to PVDF-plus membrane (Osmonics Inc., Westborough, MA) at 100 volts for one hour. Blocking, washing and stripping solutions were prepared as suggested by manufacturer for optimal results with the ECL Plus Western Blotting Detection Reagents Kit (Amersham Biosciences, Buckinghamshire, UK). All wash steps were performed in triplicate for 10 min in Tris-buffered-saline-Tween (TBS-T). Membranes were blocked for one hour at RT in TBS-T containing 10% horse serum. The membrane was probed using heme oxygenase-1 (HO-1) antibody (2.0 μg/ml of monoclonal 34.6 kDa antibody ab13248, Abcam, Cambridge, MA) applied overnight at 4°C. Secondary antibody (peroxidase-conjugated AffiniPure goat anti-mouse IgG, Jackson ImmunoResearch Laboratories, Inc.,

West Grove, PA) was diluted 1:40,000 in TBS-T and applied for 30 min at RT. The membrane was re-probed using glutamate cysteine ligase catalytic subunit (GCLC) antibody (2.5 μg/ml of rabbit polyclonal 73 kDa antibody ab17926, Abcam) applied for 2.5 h at RT. Secondary antibody (goat polyclonal to rabbit IgG, ab6721, Abcam) was diluted 1:40,000 in TBS-T and applied for 30 min at RT. Glutamate cysteine ligase regulatory subunit (GCLM) and GCL holoenzyme levels were detected as described previously [37].

### Luciferase activity

AREc32 cells were cultured in 12-well plates to ~60% confluence and incubated in the presence of 10–20 μM of HCs or chrysin for 18 h. In some experiments, the cells were preincubated with the antioxidants NAC or MnTDE-1,3-IP$^{5+}$, or inhibitors of JNK (SP600125), p38MAPK (SB203580), PI3K (wortmannin) or ERK (U0126) for 30 min followed by exposure to HCs or chrysin. The treated cells were washed with PBS and lysed with cell lysis buffer (BD Biosciences, San Jose, CA). The cell lysate was centrifuged at 20,000 *g* for 15 min and the supernatant was used for the assay of firefly luciferase. Luciferase assays were carried out using enhanced luciferase assay kit (BD Biosciences) on a Moonlight 2010 luminometer [38]. In the case of 16HBE cells transfected with Gal4-c-Jun reporter system and treated with 2′,5′-DHC and/or MnTDE-1,3-IP$^{5+}$, activities of firefly and renilla luciferases were measured in cell lysates using a dual luciferase assay kit (Promega, Madison, WI).

### Immunoblotting of phospho-c-Jun and c-Jun

Cells were grown in 6-well plates and, after treatment, washed with PBS. Cells were then scraped in 75 mammalian protein extraction reagent (M-PER, Pierce, Rockford, IL) supplemented with phosphatase inhibitors (20 mM of sodium fluoride, 1 mM of sodium orthovanadate and 500 nM of okadaic acid ) and protease inhibitor cocktail. Following freeze and thaw, cell debris was spun down and the supernatant volume reduced to approximately 30 μl using microcon-10 (Amicon) tubes for 20–30 min at 4°C at 15,000 *g*. The resulting cytosolic proteins were run and transferred to a membrane as described above. Membranes were blocked for one hour at room temperature in TBS-T plus 5% milk. The membrane was probed using phospho-c-Jun antibody (#9161, Cell Signaling Technology, Inc., Danvers, MA), diluted 1:1000 in TBS-T with 5% BSA and applied overnight at 4°C. Secondary antibody (anti-rabbit IgG HRP-linked antibody, #7074, Cell Signaling Technology, Inc.) was diluted 1:1000 in TBS-T with 5% and applied for 1 h at room temperature. The membrane was re-probed using c-Jun rabbit antibody (#9165, Cell Signaling Technology, Inc.), diluted 1:1000 in TBS-T with 5% BSA and applied overnight at 4°C. The secondary antibody was the same.

### Statistical analysis

Data are presented as means ± standard error. Each experimental group consisted of three to four wells and the results repeated at least once. Data were subsequently analyzed for significant differences using ANOVA analysis coupled with a Tukey's range test where significance was preset at $P < 0.05$ (Prizm v.4, GraphPad, San Diego, CA).

## Results

### 2′,5′-DHC-induced cytotoxicity is inhibited by MnTDE-1,3-IP$^{5+}$

We tested the ability of the catalytic antioxidant MnTDE-1,3-IP$^{5+}$ to protect AREc32 cells from 2′,5′-DHC-mediated injury in order to assess the relevance of ROS in 2′,5′-DHC-induced cytotoxicity. 2′,5′-DHC started to show significant cytotoxicity at 20 μM after 48 h treatment (not shown). MnTDE-1,3-IP$^{5+}$ (10–20 μM) protected the cells against 2′,5′-

DHC-induced toxicity (40 μM), while the inhibitor of GSH synthesis L-*S*,*R*-buthionine sulfoximine (BSO, 20 μM) [39] noticeably increased it (Fig. 2A). Interestingly, the stochiometric antioxidant *N*-acetylcysteine (NAC, 5 mM) did not protect the cells against 2′,5′-DHC-induced cytotoxicity. As shown by microscopy using MitoSOX, AREc32 cells treated for 24 h with 2′,5′-DHC (40 μM) showed an increase ROS levels (Fig. 2B), while this effect was diminished when cells were co-treated with MnTDE-1,3-IP$^{5+}$ (10 μM). A non-toxic concentration of 2′,5′-DHC (10 μM) was then analyzed for its ability to increase ROS production over time (1, 3, 6 and 24 h treatment) by flow cytometry. 2′,5′-DHC (10 μM) induced a burst of ROS at 1 h treatment (Fig. 2C), while the responses at longer treatment times (3, 6 and 24 h treatment) where closer to control (not shown).

### 2′,5′-DHC induces a biphasic modulation of intracellular GSH levels

In order to examine the role of ROS in triggering the 2′,5′-DHC-induced increase in iGSH levels, the response of the cells was examined over time using non-toxic concentrations of 2′,5′-DHC and MnTDE-1,3-IP$^{5+}$ (10 μM, respectively). The response of the cells to 2′,5′-DHC treatment was biphasic with 2′,5′-DHC inducing a significant drop (6 h) followed by a sharp increase (24 h) in iGSH levels (Fig. 3A). In contrast, chrysin (Fig. 1) induced a drop in iGSH levels with no iGSH rebound. MnTDE-1,3-IP$^{5+}$ significantly inhibited the 2′,5′-DHC-induced increase in iGSH levels (Fig. 3B), suggesting that the response is mediated by ROS. In contrast, the precursor of GSH synthesis NAC (1 mM) further increased iGSH levels, presumably by increasing cysteine availability. When compared to 2′,5′-DHC, the non-hydroxylated chalcone and 2′-HC had intermediate effects in inducing increased iGSH levels (chalcone < 2′-HC < 2′,5′-DHC) (Fig. 3C), indicating a role for the hydroxyl groups.

### 2′,5′-DHC induces increased synthesis of GSH

To test whether the HC-induced increase in iGSH levels was due to increased GSH synthesis, protein extracts of 2′,5′-DHC-treated cells were analyzed for their ability to catalyze the formation of γ-glutamyl-cysteine (γ-GC). This reaction is catalyzed by glutamate cysteine ligase (GCL), the rate-limiting enzyme in the overall synthesis of GSH [16]. 2′,5′-DHC treatment (15 μM, 16 h) increased GCL activity by 20% (Fig. 4A). A common marker of antioxidant adaptive responses is the expression of the antioxidant enzyme heme oxygenase-1 (HO-1) [19]. Cytosolic fractions of 2′,5′-DHC-treated AREc32 cells were analyzed by immunoblotting for both the catalytic subunit of GCL (GCLC) and HO-1. MnTDE-1,3-IP$^{5+}$ (10 μM) clearly inhibited the 2′,5′-DHC-induced expression of HO-1 (Fig. 4B). However, we could not detect an up-regulation of GCLC or GCLM, nor an increase in GCL holoenzyme formation in 2′,5′-DHC-treated cells (Fig. 4C).

### 2′,5′-DHC induces the Nrf2/ARE transcriptional response

In order to determine whether HCs induce the activation of the Nrf2/ARE response, the luciferase activity of AREc32 cells was measured after 18 h treatment with HCs. 2′-HC and 2′,5′-DHC (10–20 μM) clearly induced a Nrf2/ARE response (Fig. 5A). Higher concentrations did not significantly increase the effect, reaching a plateau at 20 μM (not shown). The intensity of the response induced by the non-hydroxylated chalcone (10–20 μM) was lower as compared to 2′-HC (Table 1). These data shows that hydroxyl groups in the chalcone moiety improve, but are not crucial for the Nrf2/ARE response. Compared to the chalcones, chrysin had only a modest effect (Table 1). The HCs-induced Nrf2/ARE response was not inhibited by NAC (5 mM) nor by MnTDE-1,3-IP$^{5+}$ (10 μM) (Fig. 5B), indicating that the Nrf2/ARE response is not dependent on ROS. The latter result also confirms that MnTDE-1,3-IP$^{5+}$ does not interfere with 2′,5′-DHC transport into the cell.

### 2′,5′-DHC-induced Nfr2/ARE response activity is mediated by p38MAPK and JNK

In order to examine the signaling pathways that are involved in the 2′,5′-DHC-induced Nrf2/ARE response, pharmacological inhibitors of various protein kinase pathways were used, namely SP600125, SB203580, wortmannin and U0126 for the JNK, p38MAPK, PI3K, and ERK pathways, respectively [21]. Treatment of cells with SP600125 (20 μM) or SB203580 (20 μM) inhibited 2′,5′-DHC-induced luciferase activity by 43% and 61%, respectively, while wortmannin (100 nM) had no significant effect (Fig. 6A–C). Interestingly, U0126 (10 μM) itself induced Nrf2/ARE activity which was enhanced by 2′,5′-DHC (Fig. 6D). SB203580 (20 μM), SP600125 (20 μM) and wortmannin (100 nM) were also tested in their ability to inhibit 2′,5′-DHC-induced GSH synthesis (24 h treatment). SB203580 and SP600125 inhibited the 2′,5′-DHC-induced increase in iGSH (Fig. 6E), while wortmannin had a partial inhibitory effect. U0126 (10 μM) alone or in combination with 2′,5′-DHC had no significant effects on iGSH levels (not shown). Overall, these results show that 2′,5′-DHC-induced Nrf2/ARE activity involves p38MAPK and JNK, and suggest a possible but less important role for PI3K.

### 2′,5′-DHC-induced phosphorylation of c-Jun is ROS-dependent

Previous studies have shown that JNK mediates the activation of both the Nrf2/ARE and AP-1 transcriptional responses [17–19]. In order to determine whether 2′,5′-DHC-induced activation of the JNK pathway was mediated by ROS, AREc32 cells were treated with 2′,5′-DHC (15 μM) and/or MnTDE-1,3-$IP^{5+}$ (10 μM) for 2 h and analyzed by immunoblotting. 2′,5′-DHC induced the phosphorylation of c-Jun and this effect was inhibited by MnTDE-1,3-$IP^{5+}$ (Fig. 7A). To examine this further, cultured 16HBE cells were transiently transfected with a luciferase reporter gene driven by four copies of the Gal4 regulatory sequence (pGal4-TK-Luc) along with the expression vector for the chimeric protein Gal4-c-Jun, which is activated by JNK-mediated phosphorylation of c-Jun. 2′,5′-DHC (30 μM) induced c-Jun-responsive luciferase reporter activity (24 h treatment), an effect that was inhibited by MnTDE-1,3-$IP^{5+}$ (20 μM) (Fig. 7B). This data confirms in another cell line the ROS-dependent activation of the JNK pathway by 2′,5′-DHC.

## Discussion

Our results demonstrate that non-toxic concentrations of 2′,5′-DHC induce a burst of ROS (Fig. 2A and 2B), which plays a crucial role in triggering an increase in iGSH levels, as shown using the catalytic antioxidant MnTDE-1,3-$IP^{5+}$ (Fig. 3B). Moreover, ROS are involved in triggering the AP-1 transcriptional response, as shown using the inhibitor of the JNK pathway SP600125 (Fig. 6E), immunoblotting of phospho-c-Jun (Fig. 7A) and c-Jun responsive reporter activity (Fig. 7B). However, while JNK and p38MAPK were important mediators of 2′,5′-DHC-induced Nrf2/ARE transcriptional activity and the increase in iGSH levels (Figs. 6A, 6B and 6E), activation of this pathway appeared independent from ROS production (Fig. 5B). Our findings suggest that 2′,5′-DHC induces an increase in iGSH levels through at least two transcriptional pathways: 1) a ROS-dependent and JNK-mediated activation of the AP-1 transcriptional response, and; 2) a ROS-independent and JNK- and p38MAPK-mediated activation of the Nrf2/ARE transcriptional response. Previous studies suggest that induction of HO-1 expression by 2′-HC and by synthetic chalcone and curcumin analogs involves the PI3K pathway [24,25,40]. Our results also indicate that this pathway is involved in the 2′,5′-DHC-induced increase in iGSH levels, but to a lesser extent than the JNK and p38MAPK pathways (Figs. 6C and 6E).

The 2′,5′-DHC-induced increase in iGSH levels (Figs. 3 and 7) was accompanied by a small (~20%) but significant increase in GCL enzymatic activity (Fig. 4A). Surprisingly, while the relative levels of the GCL subunits are a major determinant of cellular GCL

activity and both GCL subunits are highly regulated at the transcriptional level [16], 2′,5′-DHC-induced Nrf2/ARE and AP-1 transcriptional activity was not accompanied by an increase in GCL subunit expression levels (Fig. 4B). Increased GCL holoenzyme formation could also account for the increased GCL activity. Indeed, we and others have demonstrated that oxidative stress can increase GCL holoenzyme formation and/or GCL activity in the absence of increased GCL subunit protein expression [41–43]. However, no increase in GCL holoenzyme was detected in response to 2′,5′-DHC treatment (Fig. 4C). Such findings suggest that 2′,5′-DHC-induced GCL activity may involve a post-translational regulatory mechanism [16]. We have recently demonstrated that 4-hydroxy-2-nonenal (4-HNE), an α,β-unsaturated aldehyde produced during lipid peroxidation, can activate GCLC via direct covalent modification [37]. However, it remains to be determined whether 2′,5′-DHC-induced ROS production is associated with increased lipid peroxidation and formation of 4-HNE. 2′,5′-DHC may also increase GCL activity by altering GCL enzyme kinetics by a mechanism independent of GCL holoenzyme formation, such as GSH negative feedback regulation or increased cysteine availability. Consistent with this hypothesis, 2′,5′-DHC induces a transient reduction in iGSH (Fig. 3), which could increase GCL activity by relieving the negative feedback regulation of GCL by GSH [44]. Nrf2 also regulates the expression of the Xc- glutamate/cystine antiporter [45] and 2′,5′-DHC-induced Nrf2/ARE activity could increase Xc- expression and indirectly enhance GSH biosynthesis via increased cysteine uptake and availability. Irrespective of the molecular mechanism(s) mediating 2′,5′-DHC-induced activation of GCL, it is likely that additional mechanisms contribute to the increase in iGSH. In this regard, increased iGSH could result from increased glutathione synthetase (GS) activity and/or decreased utilization or reduced extrusion of iGSH. Interestingly, many enzymes involved in the synthesis, metabolism, and export of GSH are regulated by Nrf2 [45]. Thus, while it is unclear why increased Nrf2/ARE and/or AP-1 activity in response to 2′,5′-DHC does not result in increased GCL subunit expression in this cell system, increased GCL activity in conjunction with other molecular mechanisms are likely to account for the increase in iGSH.

Several structure-activity relationship studies have been previously carried out on the ability of HCs and synthetic analogs to: 1) inhibit the synthesis of the inducible nitric oxide (NO) synthase and induce the expression of heme oxygenase-1 (HO-1) [23–25,46]; 2) inhibit P-glycoprotein- and BCRP-mediated xenobiotic efflux [47–49], and; 3) induce GSH efflux [8,9]. However, while antioxidant adaptive responses have been examined for curcumin, some flavonoids and other polyphenols [21,50,51], the ability of 2′,5′-DHC to increase iGSH levels was never previously examined. Chrysin and other flavonoids are known to trigger GSH efflux through MRP1 and to inhibit BCRP-mediated drug efflux [11,52]. In contrast, 2′,5′-DHC-induced GSH efflux is mediated by BCRP/ABCG2 and naturally occurring chalcones are poor inhibitors of BCRP-mediated drug efflux [12,52]. Another relevant difference between 2′,5′-DHC and chrysin is that only 2′,5′-DHC is able to induce a significant rebound in iGSH levels, as shown in this study. The evidence associating aging-related diseases with oxidative stress is mounting, renewing the interest in understanding the mechanisms of the antioxidant adaptive responses [53–55]. However, as the data increases, so does the complexity of the system. The Nrf2/ARE transcriptional pathway is most studied by its known triggers, which include oxidative stress, electrophiles and multiple protein kinase signaling pathways, yet ROS may or may not be required [17,18,20,21]. Cross-talk between pathways is also at play, since JNK- and ERK-mediated pathways have been associated with both Nrf2/ARE and AP-1 transcriptional responses [17–19]. Recent results showed a synergistic effect between several natural compounds, and that such effects rely on several signaling pathways [21,56]. Further studies are needed to determine whether hydroxychalcones can contribute to similar synergistic effects.

## Acknowledgments

This work was supported by NIH grants HL755223, HL84469, ES015678 and ES017582 to B. J. Day, and VA Merit Review NEUD-004-07F to S. Pugazhenthi. The authors thank Gregory Mahaffey for his help with immunoblotting. Dr. Day is a consultant for and holds equity in Aeolus Pharmaceuticals that is commercially developing metalloporphyrins as human therapeutic agents.

## Abbreviations

| | |
|---|---|
| **AP-1** | activator protein-1 |
| **ARE** | antioxidant response element |
| **BCRP** | breast cancer resistance protein |
| **BSO** | L-buthionine sulfoximine |
| **2′,5′-DHC** | 2′,5′-dihydroxychalcone |
| **ERK** | extracellular-signal-regulated kinase |
| **GCLC** | glutamate cysteine ligase catalytic subunit |
| **GCLM** | glutamate cysteine ligase regulatory subunit |
| **GSH** | reduced glutathione |
| **HO-1** | heme oxygenase-1 |
| **2′-HC** | 2′-hydroxychalcone |
| **HCs** | hydroxychalcones |
| **HPLC-EC** | HPLC with electrochemical detection |
| **JNK** | c-Jun N-terminal kinase |
| **LDH** | lactate dehydrogenase |
| **MAP** | mitogen-activated protein |
| **MnTDE-1,3-IP$^{5+}$** | manganese(III) *meso*-tetrakis(*N,N′*-diethylimidazolium-2-yl)porphyrin |
| **MRP** | multidrug resistance-associated protein |
| **NAC** | *N*-acetylcysteine |
| **PI3K** | phosphatidylinositol 3-kinase |
| **ROS** | reactive oxygen species |
| **Nrf2** | NF-E2-related factor-2 |

## References

1. Lawrence NJ, McGown AT. The chemistry and biology of antimitotic chalcones and related enone systems. Curr Pharm Des. 2005; 11:1679–1693. [PubMed: 15892668]
2. Dimmock JR, Elias DW, Beazely MA, Kandepu NM. Bioactivities of chalcones. Curr Med Chem. 1999; 6:1125–1149. [PubMed: 10519918]
3. Go ML, Wu X, Liu XL. Chalcones: an update on cytotoxic and chemoprotective properties. Curr Med Chem. 2005; 12:481–499. [PubMed: 15720256]
4. Cheng JH, Hung CF, Yang SC, Wang JP, Won SJ, Lin CN. Synthesis and cytotoxic, anti-inflammatory, and anti-oxidant activities of 2′,5′-dialkoxylchalcones as cancer chemopreventive agents. Bioorg Med Chem. 2008; 16:7270–7276. [PubMed: 18606546]

5. Nam NH, Kim Y, You YJ, Hong DH, Kim HM, Ahn BZ. Cytotoxic 2′,5′-dihydroxychalcones with unexpected antiangiogenic activity. Eur J Med Chem. 2003; 38:179–187. [PubMed: 12620662]
6. Hodnick, WF.; Ahmad, S.; Pardini, RS. Induction of oxidative stress by redox active flavonoids. In: Manthey, JA.; Buslig, BS., editors. Flavonoids in the living system. New York: Plenum Press; 1998. p. 131-150.
7. Tomecková V, Guzy J, Kusnír J, Fodor K, Mareková M, Chavková Z, Perjési P. Comparison of the effects of selected chalcones, dihydrochalcones and some cyclic flavonoids on mitochondrial outer membrane determined by fluorescence spectroscopy. J Biochem Biophys Methods. 2006; 69:143–150.
8. Sabzevari O, Galati G, Moridani MY, Siraki A, O'Brien PJ. Molecular cytotoxic mechanisms of anticancer hydroxychalcones. Chem-Biol Interact. 2004; 148:57–67. [PubMed: 15223357]
9. Kachadourian R, Day BJ. Flavonoid-induced glutathione depletion: potential implications for cancer treatment. Free Radic Biol Med. 2006; 41:65–76. [PubMed: 16781454]
10. Leitner HM, Kachadourian R, Day BJ. Harnessing drug resistance: using ABC transporter proteins to target cancer cells. Biochem Pharmacol. 2007; 74:1677–1685. [PubMed: 17585883]
11. Ballatori N, Hammond CL, Cunningham JB, Krance SM, Marchan R. Molecular mechanisms of reduced glutathione transport: role of the MRP/CFTR/ABCC and OATP/SLC21A families of membrane proteins. Toxicol Appl Pharmacol. 2005; 204:238–255. [PubMed: 15845416]
12. Brechbuhl HM, Gould N, Kachadourian R, Riekhof WR, Voelker DR, Day BJ. The breast cancer resistance protein (ABCG2/BCRP) is a novel glutathione transporter. J Biol Chem. 2010; 285:16582–16587. [PubMed: 20332504]
13. Kachadourian R, Leitner HM, Day BJ. Selected flavonoids potentiate the toxicity of cisplatin in human lung adenocarcinoma cells: a role for glutathione depletion. Inter J Oncol. 2007; 31:161–168.
14. Ferrándiz ML, Devesa I. Inducers of heme oxygenase-1. Curr Pharm Des. 2008; 14:473–486. [PubMed: 18289074]
15. Forman HJ, Zhang H, Rinna A. Glutathione: overview of its protective roles, measurement, and biosynthesis. Mol Aspects Med. 2009; 30:1–12. [PubMed: 18796312]
16. Franklin CC, Backos DS, Mohar I, White CC, Forman HJ, Kavanagh TJ. Structure, function, and post-translational regulation of the catalytic and modifier subunits of glutamate cysteine ligase. Mol Aspects Med. 2009; 30:86–98. [PubMed: 18812186]
17. Li W, Kong AN. Molecular mechanisms of Nrf2-mediated antioxidant response. Mol Carcinog. 2009; 48:91–104. [PubMed: 18618599]
18. Itoh K, Tong KI, Yamamoto M. Molecular mechanism activating Nrf2-Keap1 pathway in regulation of adaptive response to electrophiles. Free Radic Biol Med. 2004; 36:1208–1213. [PubMed: 15110385]
19. Vesely PW, Staber PB, Hoefler G, Kenner L. Translational regulation mechanisms of AP-1 proteins. Mutat Res. 2009; 682:7–12. [PubMed: 19167516]
20. Baglole CJ, Sime PJ, Phipps RP. Cigarette smoke-induced expression of heme oxygenase-1 in human lung fibroblasts is regulated by intracellular glutathione. Am J Physiol Lung Cell Mol Physiol. 2008; 295:L624–636. [PubMed: 18689604]
21. Velmurugan K, Alam J, McCord JM, Pugazhenthi S. Synergistic induction of heme oxygenase-1 by the components of the antioxidant supplement Protandim. Free Radic Biol Med. 2009; 46:430–440. [PubMed: 19056485]
22. Liu YC, Hsieh CW, Wu CC, Wung BS. Chalcone inhibits the activation of NF-kappaB and STAT3 in endothelial cells via endogenous electrophile. Life Sci. 2007; 80:1420–1430. [PubMed: 17320913]
23. Foresti R, Hoque M, Monti D, Green CJ, Motterlini R. Differential activation of heme oxygenase-1 by chalcones and rosolic acid in endothelial cells. J Pharmacol Exp Ther. 2005; 312:686–693. [PubMed: 15537827]
24. Abuarqoub H, Foresti R, Green CJ, Motterlini R. Heme oxygenase-1 mediates the anti-inflammatory actions of 2′-hydroxychalcone in RAW 264.7 murine macrophages. Am J Physiol Cell Physiol. 2006; 290:C1092–1099. [PubMed: 16291820]

25. Ban HS, Suzuki K, Lim SS, Jung SH, Lee S, Ji J, Lee HS, Lee YS, Shin KH, Ohuchi K. Inhibition of lipopolysaccharide-induced expression of inducible nitric oxide synthase and tumor necrosis factor-alpha by 2′-hydroxychalcone derivatives in RAW 264.7 cells. Biochem Pharmacol. 2004; 67:1549–1557. [PubMed: 15041472]
26. Kachadourian R, Johnson CA, Min E, Spasojevic I, Day BJ. Flavin-dependent antioxidant properties of a new series of *meso*-*NN*′, -dialkyl-imidazolium substituted manganese(III) porphyrins. Biochem Pharmacol. 2004; 67:77–85. [PubMed: 14667930]
27. Castello P, Drechsel DA, Day BJ, Patel M. Inhibition of mitochondrial hydrogen peroxide production by lipophilic metalloporphyrins. J Pharmacol Exp Ther. 2008; 324:970–976. [PubMed: 18063723]
28. Ferrer-Sueta G, Hannibal L, Batinic-Haberle I, Radi R. Reduction of manganese porphyrins by flavoenzymes and submitochondrial particles: a catalytic cycle for the reduction of peroxynitrite. Free Radic Biol Med. 2006; 41:503–512. [PubMed: 16843831]
29. Wang XJ, Hayes JD, Wolf CR. Generation of stable antioxidant response element-driven reporter gene cell line and its use to show redox-dependent activation of Nrf2 by cancer chemotherapeutic agents. Cancer Res. 2006; 66:10983–10994. [PubMed: 17108137]
30. Pugazhenthi S, Phansalkar K, Audesirk G, Cabell L. Differential regulation of c-Jun and CREB by acrolein and 4-hydroxynonenal. Free Radic Biol Med. 2006; 40:21–34. [PubMed: 16337876]
31. Bernhard D, Schwaiger W, Crazzolara R, Tinhofer I, Kofler R, Csordas A. Enhanced MTT-reducing activity under growth inhibition by resveratrol in CEM-C7H2 lymphocytic leukemia cells. Cancer Lett. 2003; 195:193–199. [PubMed: 12767528]
32. Day BJ, Shawen S, Liochev SI, Crapo JD. A metalloporphyrin superoxide dismutase mimetic protects against paraquat-induced endothelial cell injury in vitro. J Pharmacol Exp Ther. 1995; 275:1227–1232. [PubMed: 8531085]
33. Julian D, April KL, Patel S, Stein JR, Wohlgemuth SE. Mitochondrial depolarization following hydrogen sulfide exposure in erythrocytes from a sulfide-tolerant marine invertebrate. J Exp Biol. 2005; 208:4109–4122. [PubMed: 16244170]
34. Zielonka J, Hardy M, Kalyanaraman B. HPLC study of oxidation products of hydroethidine in chemical and biological systems: ramifications in superoxide measurements. Free Radic Biol Med. 2009; 46:329–338. [PubMed: 19026738]
35. Bode, AM.; Rose, RC. Analysis of water-soluble antioxidants by high-performance liquid chromatography with electrochemical detection. In: Packer, L., editor. Oxidants and antioxidants, part A Methods in enzymology. Vol. 299. San Diego: Academic Press; 1999. p. 77-83.
36. Liu RM, Gao L, Choi J, Forman HJ. γ-Glutamylcysteine synthetase: mRNA stabilization and independent subunit transcription by 4-hydroxy-2-nonenal. Am J Physiol. 1998; 275:L861–869. [PubMed: 9815102]
37. Backos DS, Fritz KS, Roede JR, Petersen DR, Franklin CC. Posttranslational modification and regulation of glutamate-cysteine ligase by the α,β-unsaturated aldehyde 4-hydroxy-2-nonenal. Free Radic Biol Med. 2011; 50:14–26. [PubMed: 20970495]
38. Pugazhenthi S, Nesterova A, Sable C, Heidenreich KA, Boxer LM, Heasley LE, Reusch JE-B. Akt/protein kinase B up-regulates Bcl-2 expression through cAMP response element binding protein. J Biol Chem. 2000; 275:10761–10766. [PubMed: 10753867]
39. Bailey HH. L-*S*,*R*-buthionine sulfoximine: historical development and clinical issues. Chem-Biol Interact. 1998; 111–112:239–254.
40. Pugazhenthi S, Akhov L, Selvaraj G, Wang M, Alam J. Regulation of heme oxygenase-1 expression by demethoxy curcuminoids through Nrf2 by a PI3-kinase/Akt-mediated pathway in mouse beta-cells. Am J Physiol Endocrinol Metab. 2007; 293:E645–655. [PubMed: 17535857]
41. Ochi T. Hydrogen peroxide increases the activity of c-glutamylcysteine synthetase in cultured Chinese hamster V79 cells. Arch Toxicol. 1995; 70:96–103. [PubMed: 8773181]
42. Ochi T. Menadione causes increases in the level of glutathione and in the activity of c-glutamylcysteine synthetase in cultured Chinese hamster V79 cells. Toxicology. 1996; 112:45–55. [PubMed: 8792848]

43. Krejsa CM, Franklin CC, White CC, Ledbetter JA, Schieven GL, Kavanagh TJ. Rapid activation of glutamate cysteine ligase following oxidative stress. J Biol Chem. 2010; 285:16116–16124. [PubMed: 20332089]
44. Griffith OW. Biologic and pharmacologic regulation of mammalian glutathione synthesis. Free Radic Biol Med. 1999; 27:922–935. [PubMed: 10569625]
45. Shih AY, Johnson DA, Wong G, Kraft AD, Jiang L, Erb H, Johnson JA, Murphy TH. Coordinate regulation of glutathione biosynthesis and release by Nrf2-expressing glia potently protects neurons from oxidative stress. J Neurosci. 2003; 23:3394–3406. [PubMed: 12716947]
46. Sawle P, Moulton BE, Jarzykowska M, Green CJ, Foresti R, Fairlamb IJ, Motterlini R. Structure-activity relationships of methoxychalcones as inducers of heme oxygenase-1. Chem Res Toxicol. 2008; 21:1484–1494. [PubMed: 18547064]
47. Boumendjel A, McLeer-Florin A, Champelovier P, Allegro D, Muhammad D, Souard F, Derouazi M, Peyrot V, Toussaint B, Boutonnat J. A novel chalcone derivative which acts as a microtubule depolymerising agent and an inhibitor of P-gp and BCRP in in-vitro and in-vivo glioblastoma models. BMC Cancer. 2009; 9:242. [PubMed: 19619277]
48. Han Y, Riwanto M, Go ML, Ee PL. Modulation of breast cancer resistance protein (BCRP/ABCG2) by non-basic chalcone analogues. Eur J Pharm Sci. 2008; 35:30–41. [PubMed: 18598762]
49. Liu XL, Tee HW, Go ML. Functionalized chalcones as selective inhibitors of P-glycoprotein and breast cancer resistance protein. Bioorg Med Chem. 2008; 16:171–180. [PubMed: 17964170]
50. McNally SJ, Harrison EM, Ross JA, Garden OJ, Wigmore SJ. Curcumin induces heme oxygenase-1 through generation of reactive oxygen species, p38 activation and phosphatase inhibition. Int J Mol Med. 2007; 19:165–172. [PubMed: 17143561]
51. Patel R, Maru G. Polymeric black tea polyphenols induce phase II enzymes via Nrf2 in mouse liver and lungs. Free Radic Biol Med. 2008; 44:1897–1911. [PubMed: 18358244]
52. Nicolle E, Boumendjel A, Macalou S, Genoux E, Ahmed-Belkacem A, Carrupt PA, Di Pietro A. QSAR analysis and molecular modeling of ABCG2-specific inhibitors. Adv Drug Deliv Rev. 2009; 61:34–46. [PubMed: 19135106]
53. Giudice A, Montella M. Activation of the Nrf2-ARE signaling pathway: a promising strategy in cancer prevention. Bioessays. 2006; 28:169–181. [PubMed: 16435293]
54. Prawan A, Kundu JK, Surh YJ. Molecular basis of heme oxygenase-1 induction: implications for chemoprevention and chemoprotection. Antioxid Redox Signal. 2005; 7:1688–1703. [PubMed: 16356130]
55. Son TG, Camandola S, Mattson MP. Hormetic dietary phytochemicals. Neuromolecular Med. 2008; 10:236–246. [PubMed: 18543123]
56. Zhang H, Shih A, Rinna A, Forman HJ. Resveratrol and 4-hydroxynonenal act in concert to increase glutamate cysteine ligase expression and glutathione in human bronchial epithelial cells. Arch Biochem Biophys. 2009; 481:110–115. [PubMed: 18983812]

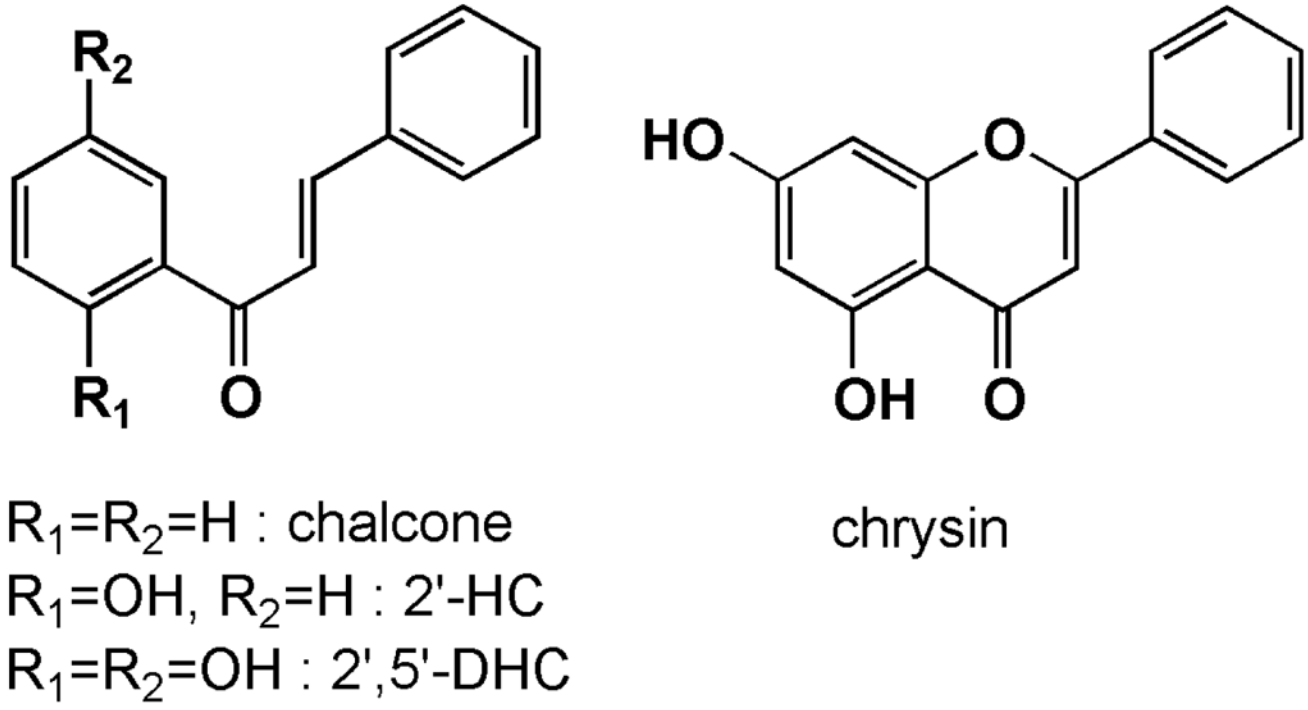


**Fig. 1.**
Structures of chalcone, 2′-hydroxychalcone (2′-HC), 2′,5′-dihydroxychalcone (2′,5′-DHC) and the flavonoid chrysin.

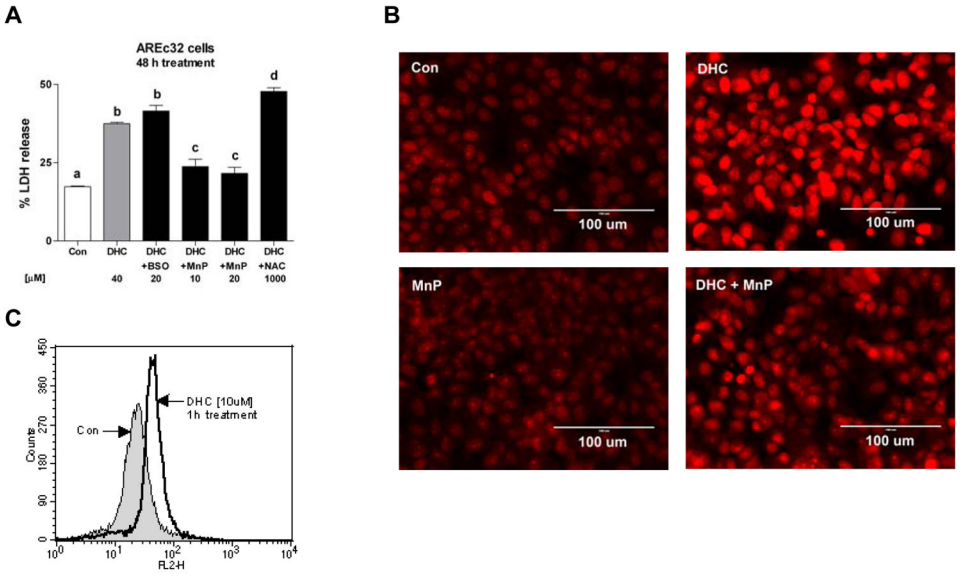


**Fig. 2.**

2′,5′-DHC induces oxidative stress. (A) 2′,5′-DHC (40 μM)-induced cytotoxicity was increased by the GSH synthesis inhibitor BSO (20 μM) and diminished by the catalytic antioxidant MnTDE-1,3-IP$^{5+}$ (MnP, 10–20 μM) (48 h treatment). *N*-acetyl cysteine (NAC, 1 mM) did not protect the cells against 2′,5′-DHC-induced cytotoxicity. Bars with different letters were statistically different from one another ($n = 4$, $P < 0.05$). (B) As shown by microscopy using MitoSOX as dye, 2′,5′-DHC (40 μM) induced an increase in ROS-induced fluorescence that was diminished by MnTDE-1,3-IP$^{5+}$ (MnP, 10 μM) (24 h treatment). (C) As shown by flow cytometry using MitoSOX as dye, a non-toxic concentration of 2′,5′-DHC (10 μM) induced a temporary increase in fluorescence at 1 h treatment ($n = 3$).

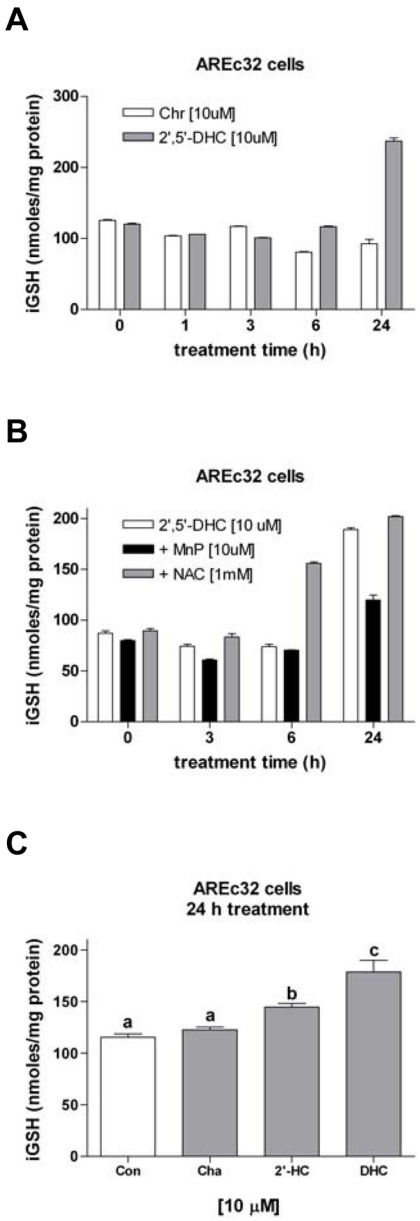


**Fig. 3.**

2′,5′-DHC-induced increase in iGSH levels is inhibited by MnTDE-1,3-IP$^{5+}$. (A) 2′,5′-DHC (10 μM) induced a drop (6 h) followed by an increase (24 h) of iGSH levels, whereas chrysin (Chr, 10 μM) induced only a drop of iGSH levels ($n = 3$). (B) MnTDE-1,3-IP$^{5+}$ (MnP, 10 μM) significantly inhibited the 2′,5′-DHC-induced increase in iGSH levels, while NAC (1 mM) did not ($n = 3$). (C) When compared to 2′,5′-DHC (DHC, 10 μM), the non-hydroxylated chalcone (Cha, 10 μM) and 2′-HC (10 μM) had intermediate effects in increasing iGSH levels. Bars with different letters were statistically different from one another ($n = 3$, $P < 0.05$).

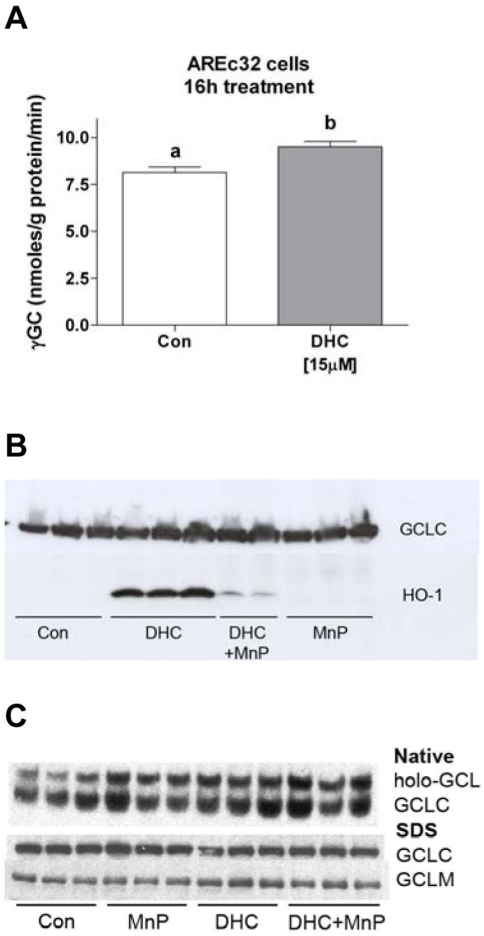


**Fig. 4.**

2′,5′-DHC induces an increase in GCL activity. (A) Cytosolic fractions of untreated (Con) and 2′,5′-DHC-treated AREc32 cells (15 μM, 16 h) were analyzed in their ability to catalyze the formation of γ-glutamyl-cysteine (γ-GC). 2′,5′-DHC induced a 20% increase in GCL activity. The reaction time was 30 min. Bars with different letters were statistically different from one another ($n = 3$, $P < 0.05$). (B) As shown by immunoblotting, 2′,5′-DHC (10 μM) induced the expression of HO-1 (34 kDa) (24 h treatment), an effect that was inhibited by MnTDE-1,3-$IP^{5+}$ (MnP, 10 μM). 2′,5′-DHC had no significant effect on GCLC (73 kDa) levels. The experiment was repeated once. (C) As shown by immunoblotting, AREc32 cells treated (24 h) with 2′,5′-DHC (10 μM) alone or in combination with MnTDE-1,3-$IP^{5+}$ (MnP, 10 μM) had no apparent effect on GCLC, GCLM nor GCL holoenzyme (holo-GCL) levels.

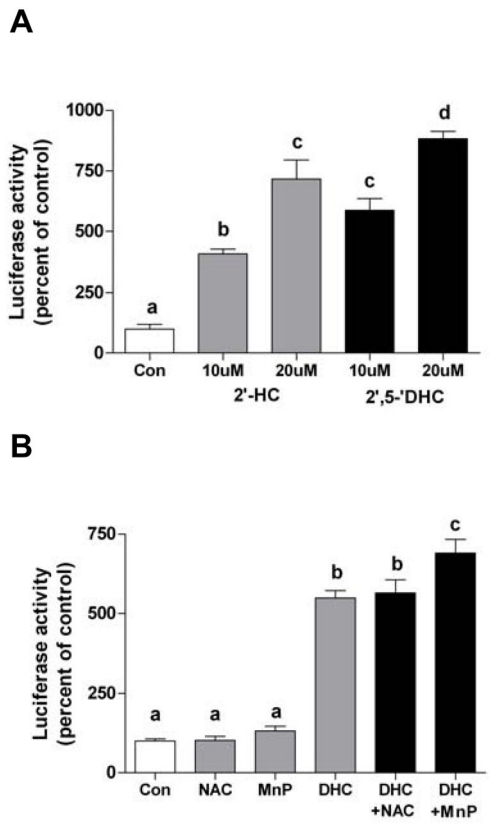


**Fig. 5.**

2′,5′-DHC-induced Nfr2/ARE response activity is ROS-independent. (A) The hydroxychalcones 2′-HC and 2′,5′-DHC (10 and 20 μM) induced the Nrf2/ARE response in AREc32 cells, as assessed by measuring luciferase activity (18 h treatment). (B) The Nrf2/ARE response was not inhibited by the antioxidants NAC (5 mM) nor MnTDE-1,3-$IP^{5+}$ (MnP, 20 μM). Bars with different letters were statistically different from one another ($n = 3$, $P < 0.05$).

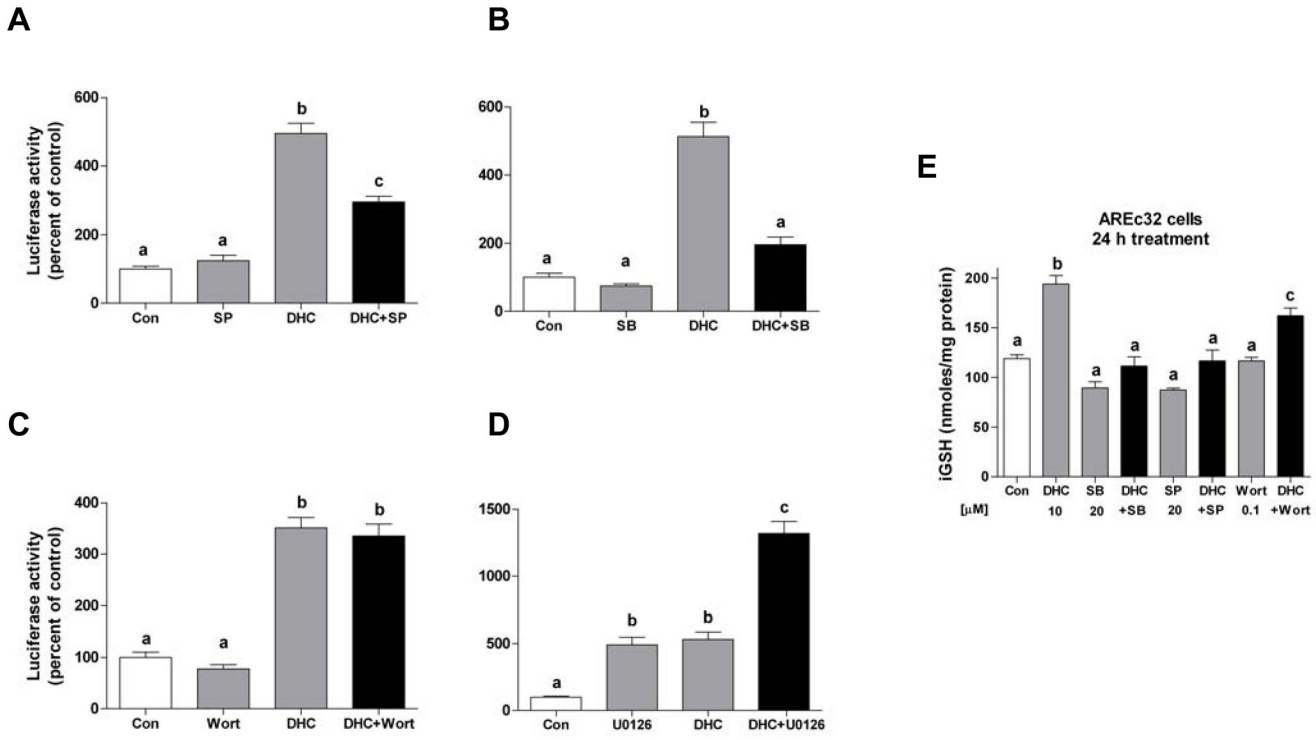


**Fig. 6.**

2′,5′-DHC-induced Nfr2/ARE response activity is inhibited by inhibitors of protein kinase pathways. (A-D) Luciferase activity was measured in 2′,5′-DHC-treated AREc32 cells co-treated with pharmacological inhibitors of various protein kinase pathways, namely SP600125 (JNK), SB203580 (p38MAPK), wortmannin (PI3K) and U0126 (ERK) (18 h treatment). (A) SP600125 (SP, 20 μM) and (B) SB203580 (SB, 20 μM) inhibited 15 μM 2′, 5′-DHC-induced luciferase activity by 43% and 61%, respectively, while (C) wortmannin (Wort, 0.1 μM) had no significant effect. (D) The inhibitor of the ERK pathway U0126 (10 μM) induced the activation of the Nrf2/ARE pathway and this effect was additive to 2′,5′-DHC co-treatment. (E) SB203580 (SB, 20 μM) and SP600125 (SP, 20 μM) and wortmannin (Wort, 0.1 μM) were tested in their ability to inhibit 2′,5′-DHC-induced GSH synthesis (24 h treatment). Both SB203580 and SP600125 had an important inhibitory effect, while wortmannin had a slight effect. Bars with different letters were statistically different from one another ($n = 3$, $P < 0.05$).

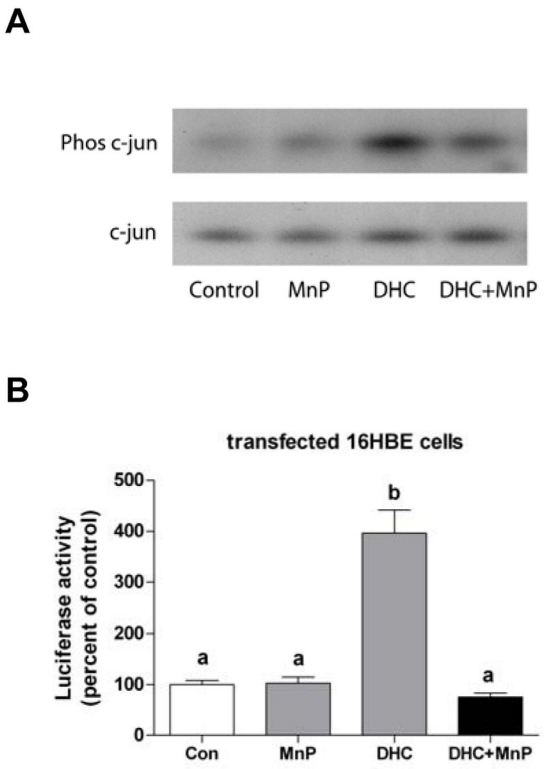


**Fig. 7.**

2′,5′-DHC-induced phosphorylation of c-Jun is ROS-dependent. (A) 2′,5′-DHC (DHC, 15 μM) induced the phosphorylation of c-Jun (48 kDa) while c-Jun levels remained the same (39 kDa) in AREc32 cells treated for 2 h, an effect that was inhibited by MnTDE-1,3-$IP^{5+}$ (MnP, 10 μM), as shown by immunoblotting. The experiment was repeated once. (B) 2′,5′-DHC (DHC, 30 μM) induced an increase in luciferase activity in transformed 16HBE cells, an effect that was inhibited by MnTDE-1,3-$IP^{5+}$ (MnP, 20 μM) (24 h treatment). Bars with different letters were statistically different from one another ($n = 3$, $P < 0.05$).

**Table 1**

Relative luciferase activity (% compared to control) in AREc32 cells treated with 2′,5′-DHC, 2′-HC, chalcone and chrysin (18 h treatment).*

| | 10 μM | 20 μM |
|---|---|---|
| 2′,5′-DHC | 596.5 ± 49.3 | 892.8 ± 36.5 |
| 2′-HC | 412.5 ± 16.5 | 717.3 ± 65.3 |
| Chalcone | 372.4 ± 40.7 | 636.3 ± 45.6 |
| Chrysin | 127.1 ± 11 | 49.7 ± 4.7** |

*Results are expressed in mean ± SEM ($n$ = 3).

**Chrysin was toxic at 20 μM.